This is to certify that the

thesis entitled

LOSS IN COMPRESSION STRENGTH OF CORRUGATED CONTAINERS AS A FUNCTION OF STACKING PATTERN AND DYNAMIC COMPRESSION

presented by

EUNGJOO KIM

has been accepted towards fulfillment of the requirements for

Masters degree in Packaging

Gary J. Burgess

Major professor

Gary J. Burgess, ph.D.

Date 4/26/93

LOSS IN COMPRESSION STRENGTH OF CORRUGATED CONTAINERS AS A FUNCTION OF STACKING PATTERN AND DYNAMIC COMPRESSION

By

Eungjoo Kim

A THESIS

Submitted to
MICHIGAN STATE UNIVERSITY
in partial fulfilment of the requirements
for the degree of

MASTER OF SCIENCE

SCHOOL OF PACKAGING

1993

ABSTRACT

LOSS IN COMPRESSION STRENGTH OF CORRUGATED CONTAINERS AS A FUNCTION OF STACKING PATTERN AND DYNAMIC COMPRESSION

By

Eungjoo Kim

This study investigated the compression strength loss of bottom containers after vibration due to different pallet patterns using three kinds of pallet patterns, corrugated boards, and package weights. This study also measured dynamic forces on the bottom box in a pallet load at resonance on a vibration table using a specially designed instrumented shipping box. The measured dynamic forces were related to measured accelerations through Newton's Law to see if the instrumented shipping box could be replaced by accelerometers. The results show that column type pallet pattern may be the strongest stacking type during long term storage but not in transit. The results also show that the dynamic forces can be accurately predicted by accelerations if there is no bouncing of individual boxes during vibration. Dynamic compression levels at resonance could not be predicted.

I would like to dedicate this thesis to

my parents: CHUNGUN KIM and CHABUN CHUNG,
for their love and prayer

my family : BYUNAH KIM (Wife) and WOOSUK KIM (Son)
for their support through this period.

ACKNOWLEDGEMENT

I wish to express my sincere gratitude to my major professor Dr. Gary J. Burgess for his expert guidance and useful suggestions. His assistance throughout my research findings is gratefully acknowledged.

I would also like to extend my sincere thanks to Dr. S. Paul Singh for his valuable advice and to Dr. Galen Brown for his help and time.

I appreciate the support of the School of Packaging, Dr. Harold A. Hughes, and Dr. Ruben J. Hernandez for offering me financial assistance as a Teaching Assistant, package consultant, and grader. I also thank Dr. Bernard Fehr and ALVCO CONTAINER CO. for their assisting in my data collection. Grateful acknowledgement is extended to Ms. Beverly Underwood for her kind help and time.

Finally, I would like to thank all the faculty and staff of the School of Packaging, all my friends, and all those who helped me in one way or another during the course of my graduate studies. They made me feel like a member of a big family while I was away from home country.

TABLE OF CONTENTS

LIST OF TABLES

LIST OF FIGURES

1.0 INTRODUCTION

The bottom package in a pallet load must be designed to withstand the maximum compression level that will occur during transportation and storage due to the load on top. Various researchers have studied the effects of static compression on packages during storage in warehouse conditions (Maltenfort, 1989). The effects of various environmental factors like creep during long term storage, temperature, humidity, and stacking pattern have been investigated. The dynamic forces that the bottom package experiences while being transported in a stack has not been previously studied.

Previous studies reveal that the column type pallet pattern is the strongest stacking pattern during long term storage compared to other types (Maltenfort, 1988). It has not yet been proven that the column type stacking pattern is also the strongest pallet pattern during transit. Therefore, the purpose of this study was to investigate the effects of different stacking patterns on the compression strength of the bottom package after it has experienced vibration during transit. An additional goal of this study was to measure the dynamic compressive forces that occur during vibration.

Three kinds of pallet patterns, corrugated boards, and

package weights were used. Boxes made from these boards were palletized and subjected to resonance tests for approximately 15 minutes. The compression strengths of the bottom boxes before and after vibration were measured. An instrumented shipping box (ISB) was also used to measure the dynamic compression levels and external accelerations.

The primary objectives of this study were to :

1. Measure the compression strength loss of bottom containers after vibration due to different pallet patterns.

2. Measure the dynamic compression forces on the bottom packages in the pallet using an instrumented shipping box specifically designed for this purpose.

3. Correlate the measured dynamic forces to accelerations measured simultaneously to see if the instrumented shipping box can be replaced by accelerometers.

2.0 Literature Review

A board for any corrugated box can be selected based on the anticipated stacking load which the box may have to support during shipment and warehousing. In making this decision, it is assumed that no abnormal influences will act upon the container, thereby claiming a share of the potential stacking strength. While it is impossible to anticipate the exact magnitude of these influences, an understanding of their effect is valuable in deciding on how strong the box should be.

A considerable amount of work has been done to determine the structural behavior of a corrugated box (Maltenfort,1988). Top-to-bottom compression strength of a single regular slotted container (RSC) can now be accurately predicted based either on material strength properties of components or with the modified IPC formula using the combined board (Maltenfort, 1989).

Kellicutt found that a B-flute RSC lost 23% of its compression strength when in a three-box-high aligned stack, and 51% when a box in this stack was misaligned by 1/2 inch (Maltenfort, 1989). For A-flute boxes, he observed an 18% strength loss when the box was in a vertically stacked palletized arrangement and a 55% loss when the stacking was in an interlocking pattern. Hillenious found a 49% strength loss for A-flute containers in an interlocking stacking arrangement, but for vertical-aligned stacks, losses ranged from 13% for a single stack down to 5% for multiple stacks while palletized (Maltenfort, 1989).

An overhanging stack of boxes suffers strength losses from two sources. First, there is a loss of approximately 10% from vertical stacking and then there is an overhanging strength loss (Fibre Box Association, 1989). The latter was found to be approximately the same as that for single boxes, when related to their single or stacked box counterparts. For example, a single box overhanging one inch on two adjacent edges will suffer a 40% loss in compression strength compared to a single box on a solid surface. A stack of three boxes, aligned with respect to each other but overhung in the same manner, will compression test approximately 40% less than a non-overhung stack of three boxes. Uldis Ievans also confirmed that there is approximately a 45% strength loss when the straight stacking pattern is changed to an interlocking one (Maltenfort, 1989).

The bursting strength of combined board is a requirement of the various carrier regulations and federal specifications for shipping containers. The bursting strength of the combined board is only a general indication of the character of the materials used in manufacturing a fiber board box and has some value in this respect. On the other hand, it gives no direct information regarding the ultimate performance of the finished container and correlates very poorly, if at all, with compression strength (TAPPI T 810, 1985). Because of this, it is necessary to perform tests and reproduce the actual environment as closely as possible.

Shipping containers are exposed to complex dynamic forces when subjected to vibration present in all transportation vehicles. This is due to the random nature of the vibration (ASTM D 4728, 1987). Approximating the actual damage experienced in shipping requires subjecting the containers and contents to vibration input. Vibration tests should be based on representative field data (ASTM D 999, 1986). Exposure to vibration can affect the shipping container, its interior packaging, means of closure, and contents. Design modifications to one or more of these components may be utilized to achieve optimum performance in the shipping environment.

Resonance responses during shipment can be severe and may lead to package or product failure. The determination of the effect of the resonant frequencies of the product and package can aid in designing the proper packaging system to provide adequate protection for the product. This also provides an understanding of the product as it relates to expected transportation vibration inputs (ASTM D 3580, 1990).

Marcondes (1988) found that acceleration levels around 1.5 g's for the products were very common in less than truck load shipments. However, levels as high as 10 g's were recorded indicating severe bouncing. The average magnification factor from the input at the wheels to the truck bed was 2 for the front and 3 for the back in less-than-truck load shipments. Low natural frequency packages (below 10 Hz) showed more bouncing and larger accelerations than high natural frequency packages.

Antle (1989) found that lateral and longitudinal vibration levels in commercial truck shipments were much lower than vertical levels. At frequencies above 20 Hz, the lateral and longitudinal levels were similar to the vertical vibration levels. The heavier loaded trucks showed higher lateral and longitudinal levels compared to the lightly loaded ones.

The data acquisition system (instrumented shipping box) developed for this study is capable of measuring dynamic compression levels that packages experience when being transported in a stack (Singh and Leinberger, 1992). The dynamic compression level measurement errors were less than ±5% and the static load measurements errors were less than ±5 lbs. The maximum dynamic compression level measured in a pilot study was found to be about five times the static load when the composite truck spectrum was used to drive the vibration table.

Random vibration testing methods of shipping containers are recommended to simulate actual conditions. These methods can be divided into three types: Closed Loop-Automatic Equalization, Closed Loop-Manual Equalization, and Open Loop -Magnetic Tape (ASTM D 4728, 1987). Automatic equalization systems allow the enter of Power Spectral Density (PSD) data as the input test levels via a control panel. Manual equalization systems allow predetermined PSD data to be controlled. Magnetic tape systems enable equalized PSD data to be incorporated into the tape's original preparation. Any of these can be used to drive random vibration controllers which operate electrohydraulic vibration tables. The problem with using random vibration for this study though is that random vibration spectra are all different in intensity levels. This would make the results for dynamic compression levels and box compression strength dependent on the particular spectrum used. It is for this reason that the standard sine wave dwell test at the resonant frequency of the stack of boxes was used (ASTM D - 999).

3.0 EXPERIMENTAL DESIGN

In order to accomplish the objectives of the study, three kinds of corrugated board, package weights, and stacking patterns were selected. Standard ASTM tests for bursting strength, vibration, and compression strength were conducted. An instrumented shipping box (ISB) specially designed for measuring forces was also used. The respective packaging materials, static loads, stacking patterns, and test methods used are described in this chapter.

3.1 Instrumented Shipping Box (ISB)

3.1.1 Explanation of Features :

The instrumented shipping box used to measure instantaneous compression forces was constructed at MSU specifically for the purpose of measuring dynamic loads. It consists of electronic hardware housed inside a reinforced plywood outer container as shown in Figure 1. This instrument measures 16 x 13 x 10 inches and is designed to fit one ninth of a standard GMA pallet. The total system weighs 45 lbs and is capable of withstanding a 5000 lb compression load.

Four internal shear beam load cells are used to measure the load at each top corner of the instrument and an internal accelerometer is used to measure the acceleration history of

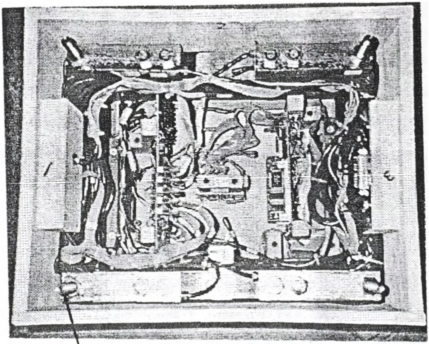

One of Four Shear Beam Load Cells

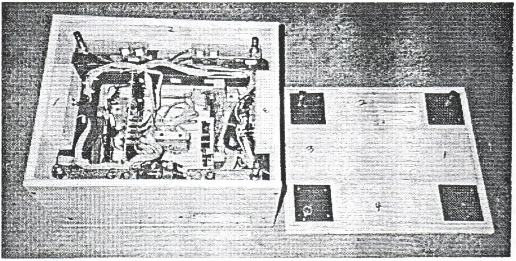

Figure 1. Instrumented Shipping Box (ISB)

the unit. The ISB has a microprocessor that is capable of accepting a maximum of 16 inputs, some of which are used for system checkouts, system status, load at each corner, internal acceleration, temperature, and humidity. The ISB also accepts a signal from an external accelerometer. The processor is capable of recording all the individual inputs at a maximum sampling rate of 200 Hz. The loads and internal and external accelerations are also measured simultaneously. All data is saved in an internal memory which can be later downloaded into a personal computer through a RS232 interface. The data can then be analyzed to determine the dynamic compression forces and external accelerations that the ISB measured.

3.1.2 Procedure for Checking the ISB Accuracy for Static Weight Measurement

The accuracy of the ISB was evaluated first using static weights. An accurate laboratory balance graduated in ounces was used to measure the weights of three metal bricks. They weighed 55.8, 53.5, 55 lbs for a combined weight of 164.3 lbs. The balance had its own errors of only ± 1/32 lbs because it was graduated in ounces. Three bricks were then placed on the ISB. A 5.5 lbs weight difference was found between the balance and the ISB (Table 1). The 32 readings shown in Table 1 are 32 successive "samples" recorded by the ISB with a sample rate of 200 Hz. Since the four internal shear beam load cells of the ISB measure the load at each top corner of the instrument by rounding up or down to the nearest pound, there is automatically a precision error of ± 2 lbs (4 x 0.5 = 2 lbs)

Table 1. Measured Static Loads and External Accelerations

No	J (lbs)	K (lbs)	L (lbs)	M (lbs)	Static Load (lbs)	External Acc(G)
1	35	49	42	33	160	0.01
2	35	49	41	35	160	0.01
3	35	47	41	35	159	0.01
4	35	47	41	32	156	0.01
5	35	47	41	33	157	0.01
6	35	46	41	35	157	0.01
7	35	46	41	32	155	0.00
8	35	46	41	35	157	0.00
9	36	47	42	35	161	0.01
10	35	46	41	33	156	0.00
11	35	47	42	33	159	0.01
12	35	47	42	35	160	0.01
13	35	47	44	33	160	0.00
14	35	46	42	35	159	0.02
15	35	47	42	33	159	0.01
16	36	47	41	33	159	0.00
17	35	47	42	33	159	0.01
18	35	47	41	33	157	0.00
19	35	47	42	35	160	0.00
20	35	47	44	32	159	0.01
21	35	47	42	33	159	0.01
22	35	47	42	35	160	0.01
23	35	49	42	35	161	0.00
24	35	49	42	33	160	0.01
25	36	47	41	33	159	0.01
26	35	47	41	33	157	0.01
27	35	47	42	35	160	0.00
28	36	47	41	33	159	0.01
29	35	47	42	32	157	0.01
30	35	49	41	35	160	0.00
31	35	49	42	33	160	0.01
32	35	47	42	36	161	0.01
AVG	35.1	47.2	41.7	33.7	158.8	0.007

* J,K,L,and M refer to the four load cells.

in the worst case. The accuracy of the ISB is taken to be ± 5.5 lbs for static weight measurements.

Table 1 also shows the 32 successive acceleration readings. The numbers represent sampling errors coming from the external accelerometer because there was no movement so the accelerations should be zero. Therefore, the external accelerometer readings have an inherent precision of ± 0.02 G.

3.1.3 Procedure for Checking the ISB Accuracy for Dynamic Force Measurement

The next check on the ISB accuracy was to estimate the error in measuring dynamic forces as opposed to static forces. This can be done in two ways. One way would be to use an external accelerometer attached to a mass which is secured to the top of the ISB. Through the use of Newton's law which relates forces to accelerations, an estimate of the dynamic measurement error of the ISB can be obtained, provided of course that the ISB is able to accurately record external acceleration. Since it is not known ahead of time that external acceleration is measured accurately, a different method was used to estimate dynamic measurement error. The application of Newton's law will then be used to estimate the error in the exact acceleration. The ability of the ISB to accurately measure dynamic forces can be evaluated by finding out how fast it responds. To do this, the natural frequency of the shear beam mechanism must be measured because the shear beam acts like a spring-mass system. If its own natural frequency is large, then it responds quickly and is very accurate for measuring dynamic events. As long as these events do not occur over time periods on the order of 1/fn where fn is equal to the natural frequency of the shear beam, then dynamic events will be recorded accurately. If the event occurs over very short time periods, then the ISB will report M times the true value:

ISB reading = M x (True force)

where M is the magnification factor(Brandenburg and Lee, 1985) defined by

$$M = 1 / [1 - (f_{event} / f_{shear\ beam})^2] \qquad 3.1$$

The natural frequency of the shear beam (Timoshenko, 1974) can be estimated using.

$$fn = 3.515 \sqrt{(EIG/DAL^4)} / 2\pi \qquad 3.2$$

where

E = modulus of elasticity = 30,000,000 lbs/in^2 for steel.

D = weight density = 0.284 lb/in^3 for steel

I = moment of inertia = $bh^3/12$ = 0.203 in^4 (b=h=1.25 in)

A = cross-section area = bh = 1.56 in^2

L = beam length = 3 in

G = acceleration due to gravity = 386.4 in/sec^2

Using these values in equation 3.2 gives

fn = 4530.1 sec^{-1} = 4530.1 Hz

Because the vibration table will be operated at frequencies characteristic of truck trailers (around 3 Hz), the magnification factor from equation 3.1 is

$$M = 1 / [1 - (3/4530.1)^2] = 1.000000439$$

Therefore, the error due to dynamic effects is around 0.00004%, which is negligible. Based on this result, the ISB should have no problem measuring dynamic forces. The error in the force reading should be the same as that for static forces.

The ISB was next tested by itself for its ability to measure external accelerations. An external accelerometer with a sensitivity of 1 mv/g and a Piezotron coupler (Kistler 5112) were used to check the ISB. A metal brick with the accelerometer attached to it was placed on top of the ISB as in Figure 2 and the table was set to vibrate at 4 Hz and 0.5 G. The ISB was set to sample at 20 Hz. The compression forces at each corner of the ISB and the acceleration of the brick were also measured simultaneously. According to Newton's second law (Figure 3), the relationship between the dynamic force F and the acceleration G should be approximately $F=(1+G)W$. The relationship $F=W(1+G)$ is not exactly correct because the weight of the platform is not accounted for. In a static weight measurement, the true static force on the shear beams is: $F = Wb + Wp$ where F is the sum of four corner shear beam forces up on platform, Wb is the weight of brick, and Wp is the weight of ISB platform. But, the ISB does not read this F value because the weight of the platform was zeroed out during calibration. Instead, it reads just Wb or F-Wp. In a

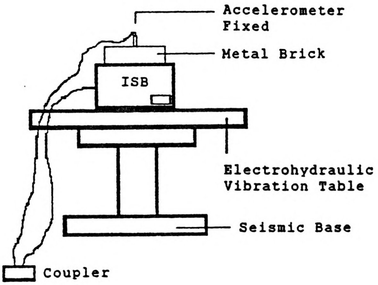

Figure 2. Test Setup for Dynamic Force Relative to Acceleration

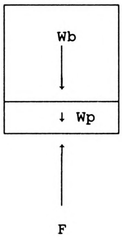

$$\Sigma F = F - Wb - Wp = WbG$$

$$\text{ISB Reading} = F - Wp$$

$$= (1+G)Wb + WpG$$

Figure 3. Newton's Second Law

or

$$F - (Wb+Wp) = (Wb+Wp)G$$

$$F = (Wb+Wp)(1+G)$$

This force (F) is the true force down on the shear beams, but this is not what the ISB reads because the weight of the platform was zeroed out. The ISB always reads an amount Wp less than the true force. In other words,

$$\text{ISB reading} = F - Wp = (Wb+Wp)(1+G) - Wp$$

$$= Wb(1+G) + WpG \qquad 3.3$$

where Wb(1+G) is the static weight of brick plus force to move brick and WpG is the force to move platform. The correct external acceleration can therefore be calculated in the following manner:

$$G = (\text{ISB force reading} - Wb) / (Wb + Wp) \qquad 3.4$$

Based on equation 3.4, Table 2 shows measured accelerations, measured forces, and actual accelerations taken over 32 successive peaks from the raw data. The measured accelerations and the actual accelerations averaged 0.4 G and 0.38 G respectively. From a statistical point of view, these two accelerations can be regarded as nearly the same value because they have large standard deviations.

The data in Table 3 was measured in the same way as the Table 2 but with a piece of expanded polyethylene cushioning between the metal brick and the ISB. This was done to measure the effect of cushioning material on measuring dynamic compression levels and external accelerations. Table 3 shows

Table 2. External Acceleration Predicted from Measured Force for Metal Brick

No	Measured Peak Acc. (G)	Measured Force(lbf)	Actual Peak Acc. (F-Wb)/(Wb+Wp)
1	0.6	87	0.46
2	0.3	73	0.24
3	0.4	85	0.43
4	0.5	86	0.45
5	0.1	75	0.27
6	0.1	73	0.24
7	0.2	75	0.27
8	0.3	73	0.24
9	0.6	87	0.46
10	0.3	87	0.46
11	0.3	62	0.07
12	0.4	86	0.45
13	0.1	74	0.26
14	0.1	75	0.27
15	0.4	85	0.43
16	0.1	73	0.24
17	0.6	86	0.45
18	0.3	86	0.45
19	0.4	85	0.43
20	0.7	88	0.48
21	0.6	87	0.46
22	0.6	88	0.48
23	0.4	86	0.45
24	0.5	86	0.45
25	0.6	87	0.46
26	0.5	83	0.40
27	0.4	71	0.21
28	0.5	85	0.43
29	0.5	85	0.43
30	0.5	85	0.43
31	0.6	86	0.45
32	0.3	83	0.40
AVG±STD	0.4±0.175	81.7±6.65	0.38±0.11

* The table was set at 0.5 G and 3Hz. The ISB was set to sample at 20Hz.

Table 3. External Acceleration Predicted from Measured Force for EPE

No	Measured Peak Acc. (G)	Measured Force(lbf)	Actual Peak Acc. (F-Wb)/(Wb+Wp)
1	0.5	92	0.54
2	0.5	92	0.54
3	0.5	90	0.51
4	0.6	94	0.57
5	0.6	91	0.52
6	0.6	89	0.49
7	0.5	94	0.57
8	0.7	90	0.51
9	0.5	92	0.54
10	0.5	91	0.52
11	0.5	91	0.52
12	0.5	92	0.54
13	0.4	94	0.57
14	0.6	82	0.38
15	0.6	93	0.57
16	0.4	88	0.48
17	0.4	81	0.38
18	0.7	91	0.52
19	0.5	97	0.62
20	0.3	92	0.54
21	0.7	92	0.54
22	0.6	89	0.49
23	0.4	94	0.57
24	0.4	93	0.56
25	0.4	92	0.54
26	0.6	92	0.54
27	0.5	91	0.52
28	0.4	92	0.54
29	0.5	93	0.56
30	0.5	91	0.52
31	0.8	92	0.54
32	0.8	92	0.54
AVG±STD	0.53±0.12	91.2±3	0.53±0.05

* Same as Table 2 but with a expanded polyethylene foam between the metal brick and the ISB.

that the measured and actual accelerations are the same on average. On the basis of the results in these two tables, it can be concluded that the external accelerometer measures accelerations accurately.

Since the relationship between force and acceleration must be true at every instant, it should not matter what the sampling rate of the ISB is. Sampling rate does matter however when the ISB is used to measure such things as peak force and peak acceleration. Therefore, an estimate of the error in measuring peak values will be made because it affects what follows.

A low sampling rate can cause the ISB to miss the peak. The worst possible situation is when two consecutive samples are on either side of the true peak as shown in Figure 4. A perfect sine wave has been used to provide an estimate even though a true sine wave was never recorded. Because the ISB and the brick were not rigidly connected to the table, the motion was smooth enough to be considered close to that of a true sine wave. The force varies over time according to

$$\text{Force} = A \sin (2\pi t/T) \qquad 3.5$$

where A is the true amplitude, t is the time, and T is the period. The reported peak is just the sine wave evaluated at $t = T/4 - \Delta t/2$ where Δt is the time between samples:

$$\begin{aligned}\text{Reported Peak} &= A \sin [2\pi(T/4 - \Delta t/2) / T] \\ &= A \sin (\pi/2 - \pi\Delta t/T) \\ &= A \cos (\pi\Delta t/T)\end{aligned}$$

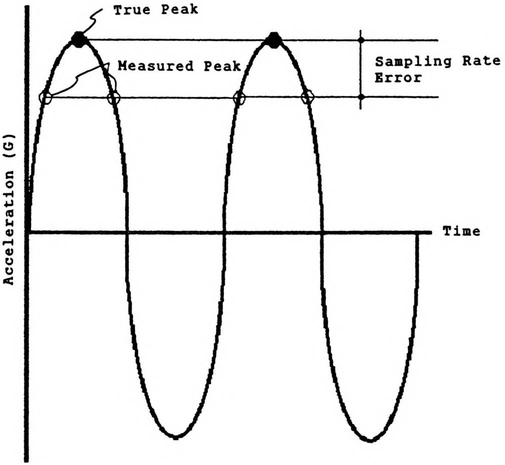

Figure 4. True Peak vs Measured Peak

The maximum percent error is defined here to be (true - reported)x100 / reported, or

$$\% \text{ error} = [A - A\cos(\pi\Delta t/T)]\text{x}100 \,/\, A\cos(\pi\Delta t/T)$$

$$= 100[\sec(\pi\Delta t/T)-1]$$

$$= 100[\sec(\pi fv/fs)-1] \qquad 3.6$$

where fv is the frequency of vibration of the table, and fs is the ISB sampling rate. Using a typical table frequency of 4 Hz and the maximum ISB sampling rate of 200 Hz, the maximum error in measuring the peak is:

Maximum error = $100[\sec(\pi 4/200) = 0.2\%$

This means that the true peak may be as much as 0.2% higher than the reported peak, but only if the table vibrates at 4 HZ and the ISB samples at 200 Hz.

Finally, the external accelerometer was used to check the vibration table. The table was set to vibrate at 4 Hz and 0.8 G peak and the ISB was set to sample at 200 Hz. The results of the external accelerometer are shown in Figure 5. The average measured acceleration was 0.82 G peak which differs from the input acceleration level by only 2.5%.

3.2 Compression Strength Loss after Vibration :

3.2.1 Materials

Two kinds of single wall "C" flute corrugated board and a "B+C" flute double wall corrugated board were used to make the test boxes for this study. All of the containers were RSC style boxes with the same external dimensions of 19.1x13.4x9.1 ±0.3 inches (length x width x height). According to the type

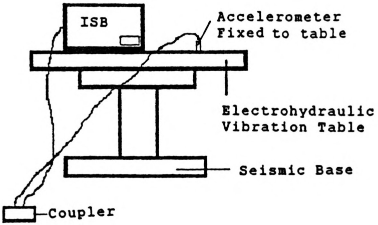

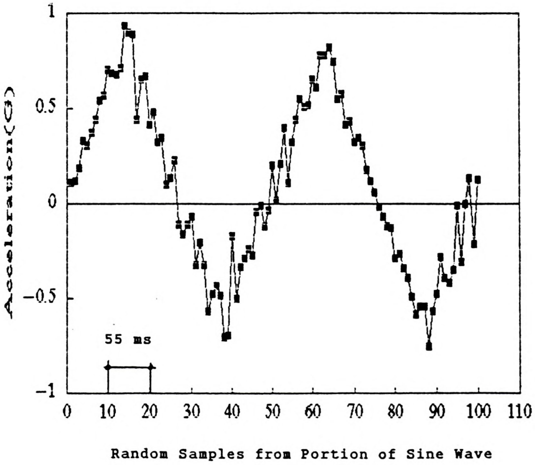

Figure 5. Test Setup and Results

of corrugated board used for the box, the boxes were designated as SW-A, SW-B, and DW which stand for single wall-board A, single wall-board B, and double wall. The specifications shown in Table 4 were taken from the manufacturer's labels shown in Figure 6. According to Rule 41 (Fibre Box Handbook, 1989), the gross weight in Figure 4 represents the maximum box weights for which no visual damage should occur. Bursting strength tests were done on samples of the board to check the manufacturer's specifications. The bursting test results using TAPPI T 810 0m-85 for ten samples are shown in Table 5.

Table 4. Corrugated Box Specifications (Fibre Box Handbook)

	SW-A	SW-B	DW
Bursting Test (lbs/in^2)	200	275	350
Min Comb Wt Facings ($lbs/1000ft^2$)	84	138	126
Size Limit (L + W + H) (inches)	75	90	100
Gross Weight (lbs)	65	90	120

* SW-A stands for Single Wall Board A, and SW-B for Single Wall Board B, and DW for Double Wall Board.

DW : "B,C" Flute

SW-A : "C" Flute

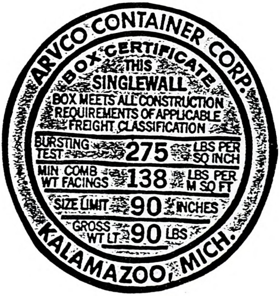

SW-B : "C" Flute

Figure 6. Box Specifications Label

3.2.2 Static Loads

Three different package weights were examined in this study. The first was 35 lbs and consisted of five house bricks tightly packed with two pieces of expanded polyethylene foam on opposite long sides with crumpled newspapers put in between all void spaces to prevent movement during vibration. The second was 52.5 lbs with eight house bricks and the third

Table 5. Measured Burst Strength (lbs/in^2)

Sample No.	SW-A	SW-B	DW
1	180	320	291
2	183	330	325
3	173	312	315
4	197	318	327
5	215	347	346
6	190	323	317
7	190	323	291
8	207	293	317
9	194	265	357
10	187	315	300
AVG ± STD	191.6±12.47	314.6±22.12	318.6±21.67

was 71 lbs with eleven house bricks. These package weights were chosen to reproduce the most common pallet load weight range of 560 lbs to 1420 lbs. These box weights exceed the Rule 41 gross weight recommendations in Table 4 only for the SW-A box with the 71 lb load.

3.2.3 Stacking Patterns

Pallet loads of these three boxes were constructed in different stacking arrangements. The various arrangements or pallet patterns are shown in Figure 7, Figure 8, and Figure 9. Each pallet pattern had four boxes per layer with four layers with the exception of the interlock pattern which had five boxes per layer. Two identical pallet loads of boxes were used so that a total of seven bottom boxes could be used for compression testing after vibration: the eighth box was unavailable because it was replaced by the ISB so that dynamic forces could be recorded. In the case of interlocking pattern where nine boxes were available, only seven were chosen so that comparisons between the other two pallet patterns could be made on a uniform basis. All boxes within a pallet load had the same weight and were made of the same corrugated board. For the SW-A board then, there were two identical pallet loads for each of the three types of pallet patterns and each of the three box weights:

SW-A :

2 pallet loads of 35 lb boxes in the column type.

2 pallet loads of 35 lb boxes in the interlock type.

2 pallet loads of 35 lb boxes in the pinwheel type.

2 pallet loads of 52.5 lb boxes in the column type.

2 pallet loads of 52.5 lb boxes in the interlock type.

2 pallet loads of 52.5 lb boxes in the pinwheel type.

2 pallet loads of 71 lb boxes in the column type.

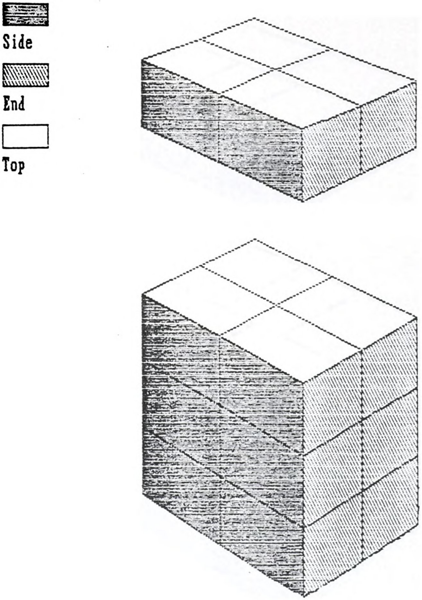

Figure 7. Column Type Pallet Pattern

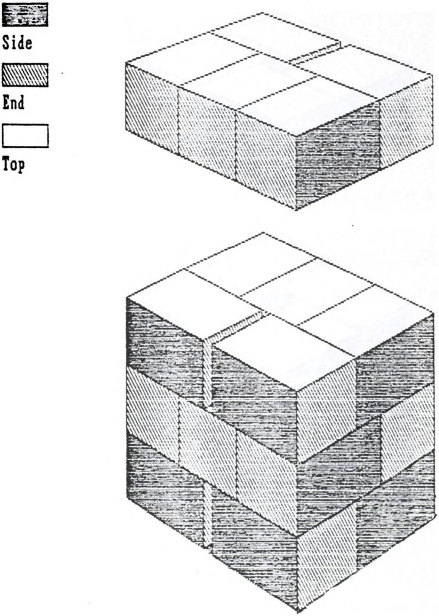

Figure 8. Interlock Type Pallet Pattern

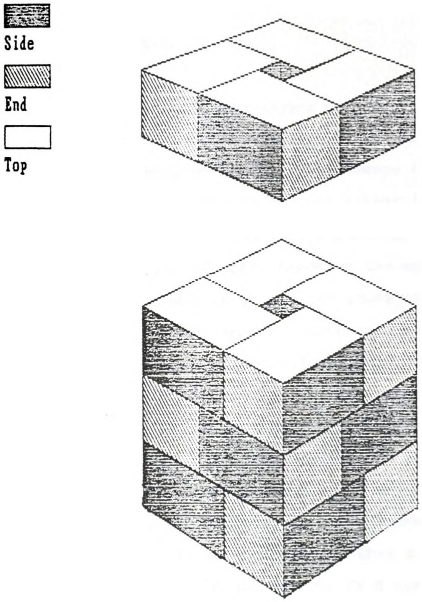

Figure 9. Pinwheel Type Pallet Pattern

2 pallet loads of 71 lb boxes in the interlock type.

2 pallet loads of 71 lb boxes in the pinwheel type.

SW-B : same as SW-A.

DW : same as SW-A.

Because there were four layers of either 35, 52.5, or 71 lb boxes in any pallet configuration, there were always three boxes on top of each bottom box. This means that the static compression load on a bottom box was either 3x35=105 lbs, 3x52,5=157.5 lbs, or 3x71=213 lbs, depending on the box weight used to make the pallet load. Based on the maximum dynamic load factor of 5 found in an earlier study (Singh and Lienberger, 1992), the dynamic compression load on a bottom box could therefore be as high as 5x105=575lbs, 5x157.5=787.5, or 5x213=1065 lbs, depending on the box weight used to reproduce the pallet load. As the compression test results in the next chapter will show the compression strengths of new boxes made from SW-A, SW-B, and DW board are around 800 lbs, 1000 lbs, and 1300 lbs respectively. The dynamic loads on the bottom boxes can therefore be greater than the static compression strengths of the SW-A and SW-B boxes. Even though the individual box weights were not intentionally chosen to make this happen, it is fortunate that it did turn out this way because it raises another important question: will a dynamic load which is greater than the static compression strength but which is presently only for short time periods on a reported basis cause the box to fail. This will be addressed

in the next chapter.

23.2.4 Vibration Tests

Vibration tests on whole pallet loads were performed on an MTS 840 electrohydraulic vibration table and a Lansmont Model 10000-10 Touchtest Vibration System. A sine sweep from 3 to 100 Hz at 0.5 G peak was used to look for resonance. The bottom boxes were packed on all four sides with expanded polyethylene foam to prevent the collapse of stacked boxes during vibration. These boxes were placed at the bottom layer on the vibration table and three layers boxes loaded with house bricks were put on the top of the bottom boxes. Pallets were not used and all boxes were conditioned at 73°F and 50 % RH for 24 hours prior to testing.

Guide rods with wooden boards fixed to them were attached to the table as restraining devices to prevent the specimens from horizontal movement off the platform, and to prevent toppling and excessive rocking. The restraining devices were adjusted to permit free movement of the test specimens to within 10 mm (0.4 in.) in any direction. The test setup is shown in Figure 10. The vibration tests were performed for approximately 15 minutes at the resonant frequency of the pallet load using a table acceleration of 0.5 G's in accordance with ASTM D-999.

3.2.5 Compression Strength Tests

The compression strength tests were performed before and after the vibration test according to ASTM D 642-90:

Determining Compressive Resistance of Shipping Containers, Components, and Unit Loads. For these tests, A Lansmont Model 1210-AF Compression Tester was used. The boxes were maintained at 73°F and 50% RH following the vibration test, and compression tested under the same conditions.

3.2.6 A Related Test

An accelerometer was attached to the middle box in the column of three boxes resting on top of the ISB. The accelerometer was taped to the side of box. The middle box was chosen because it represents the mass center of the column of boxes on the ISB. The output of the accelerometer was fed into the ISB so that it could measure acceleration and force simultaneously to see if there was in fact the expected relationship between the two. The same box weights of 35 lbs, 52,5 lbs, and 71 lbs used in the pallet load vibration tests were used in this test. The test setup is shown in Figure 11.

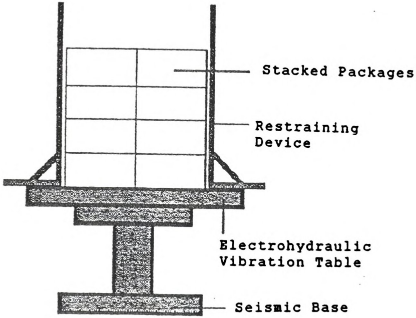

Figure 10. Test Setup for Vibration

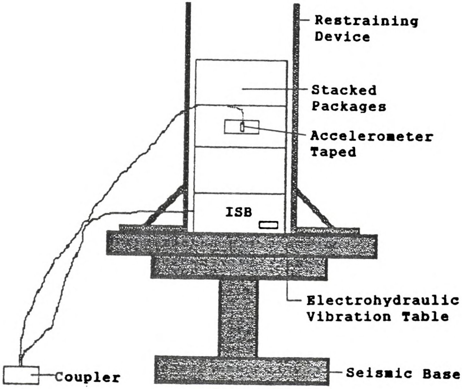

Figure 11. Test Setup for Comparing Forces and Accelerations

4.0 DATA AND RESULTS

There were two different kinds of tests performed in this study: 1)compression tests on bottom boxes in a pallet load after vibration t resonance for 15 minutes, and 2)simultaneous force and acceleration measurements on a column of boxes. The results of the force and accelerations will be presented first.

4.1 Dynamic Compression Level vs Acceleration :

4.1.1 Package Weights

The data in Table 6 shows the relationship between the actual force measured by the ISB and the predicted force using the measured acceleration and Newton's law. A box weight of 52.5 lbs was used to produce a static load of 157.7 lbs on the bottom box in a stack of three (shown in Figure 11). For this test, the vibration table was set at 3 Hz and 0.5 G and the ISB was set to sample at 20 Hz. No bouncing was found during the test. Measured forces and predicted forces averaged 230 lbs and 204 lbs respectively. From the statistical point of view, these two forces can be also regarded as a same value because they have big standard deviations. The data in Table 7 was measured in the same way as Table 6 but with a different static load of 105 lbs. The measured forces and predicted forces averaged 158 and 142 lbs respectively. This shows that measured forces weighed around 12 lbs more than that of predicted one. The data in Table 6 and 7 show that dynamic forces can similarly be predicted by measuring acceleration and applying Newton's law. An obvious consequence of this is that dynamic force measurements can be made without the need for an expensive instrument like the ISB. But the tests so far have been done in such a way that no bouncing of boxes on top of each other took place. At resonance, where bouncing will occur, there may not be such a relationship between force and acceleration.

Table 6. Measured Forces vs Predicted Forces for a 157.5 lb Static Load

No	Successive Peak Acc. (1 + G)	Measured Force(lbf)	Predicted Force(lbf) Wb(1+G)+WpG
1	1.18	209	187
2	1.29	237	205
3	1.22	244	194
4	1.19	212	187
5	1.34	241	213
6	1.26	246	200
7	1.29	209	205
8	1.38	240	220
9	1.26	244	200
10	1.28	206	203
11	1.35	238	215
12	1.26	244	200
13	1.28	207	203
14	1.33	238	211
15	1.31	246	208
16	1.33	208	211
17	1.41	240	225
18	1.18	225	187
19	1.28	207	203
20	1.41	236	225
21	1.32	248	210
22	1.37	236	218
23	1.33	242	211
24	1.30	204	207
25	1.43	238	225
26	1.35	244	215
27	1.34	207	213
28	1.47	240	235
29	1.33	241	211
30	1.34	203	213
31	1.43	235	228
32	1.37	242	218
AVG±STD	1.32	230±16.1	204±35.7

Table 7. Measured Forces vs Predicted Forces for a 105 lb Static Load

No	Successive Peak Acc. (1 + G)	Measured Force(lbf)	Predicted Force(lbf) Wb(1+G)+WpG
1	1.47	163	157
2	1.35	159	144
3	1.40	154	149
4	1.42	165	152
5	1.39	159	148
6	1.42	150	152
7	1.45	163	155
8	1.38	159	147
9	1.37	153	146
10	1.41	166	150
11	1.32	153	140
12	1.39	165	148
13	1.33	162	142
14	1.34	149	143
15	1.38	163	147
16	1.35	160	144
17	1.34	154	143
18	1.38	163	147
19	1.33	161	142
20	1.37	148	146
21	1.39	162	148
22	1.37	160	146
23	1.31	149	139
24	1.39	166	148
25	1.32	160	140
26	1.33	150	142
27	1.39	161	148
28	1.32	159	140
29	1.34	149	143
30	1.40	163	149
31	1.39	161	148
32	1.33	146	142
AVG±STD	1.37	158±5.9	146±4.3

As the table frequency approaches the natural frequency of the stack of boxes during the sweep, the value of the vibration magnification factor M increases; $M = 1 / [1 - (Ft/Fn)^2]$ where Ft stands for the table frequency and Fn for natural frequency. At the resonance where Ft/Fn = 1, the value of M becomes infinite. This means that a very small input vibration will cause an extremely large response: in other words, the stack of boxes will bounce and separation will occur.

To test the relationship between force and acceleration at resonance, a static load of 213 lbs on the bottom box was used. The vibration table frequency was adjusted so that the stack resonated. The measured forces and predicted forces averaged 402 lbs and 560 lbs respectively (Table 8). The data in Table 9 was measured in the same way as Table 8 but with a different static load of 105 lbs and a different vibration table frequency of 7.5 Hz. The measured forces and predicted forces averaged 184 lbs and 269 lbs respectively. These results show that the dynamic forces can not be predicted by measuring accelerations when there is separation between individual boxes. The reason is that Newton's law requires the acceleration to be measured at the mass center of the stack of boxes. When there is separation, the mass center is no longer located at the middle box.

Table 8. Measured Forces vs Predicted Forces for a 213 lb Static Load at Stack Resonance.

No	Successive Peak Acc. (1 + G)	Measured Force(lbf)	Predicted Force(lbf) Wb(1+G)+WpG
1	2.30	405	497
2	2.99	404	648
3	2.76	404	598
4	2.04	401	441
5	2.75	402	596
6	2.23	401	482
7	1.75	399	377
8	1.92	405	414
9	1.82	401	392
10	2.56	406	554
11	4.88	400	1062
12	3.20	401	694
13	3.15	406	683
14	2.80	405	607
15	3.53	400	766
16	1.85	406	399
17	1.57	396	338
18	1.92	400	414
19	2.61	396	565
20	1.85	401	399
21	2.57	401	556
22	3.15	402	683
23	2.94	404	637
24	4.12	402	896
25	3.01	404	653
26	2.31	398	500
27	2.93	402	635
28	2.77	396	600
29	1.83	402	395
30	2.70	402	585
31	1.63	401	351
32	2.38	400	515
AVG±STD	2.59	402±2.8	560±160.3

Table 9. Measured Forces vs Predicted Forces for a 105 lb Static Load at Stack Resonance

No	Successive Peak Acc. (1 + G)	Measured Force(lbf)	Predicted Force(lbf) Wb(1+G)+WpG
1	2.80	233	304
2	2.69	217	292
3	2.46	213	267
4	2.62	195	284
5	2.45	188	266
6	2.46	169	267
7	2.41	176	261
8	2.79	185	303
9	2.87	186	312
10	2.55	189	277
11	1.71	190	184
12	2.48	181	269
13	2.64	159	287
14	2.31	127	250
15	2.49	226	270
16	2.44	203	264
17	2.99	192	325
18	2.40	167	260
19	2.52	172	273
20	2.52	188	273
21	2.24	185	242
22	2.53	184	274
23	2.26	189	245
24	2.54	180	276
25	2.34	157	253
26	2.55	235	277
27	2.02	83	218
28	2.61	212	283
29	2.50	190	271
30	2.11	167	228
31	2.61	174	283
32	2.36	184	256
AVG±STD	2.48	184±29.0	269±26.8

4.2 Compression Strength Loss :

The seven bottom boxes in the two pallet loads of identical boxes were compression tested after 15 minutes of vibration at resonance. The results are shown in Table 10-18. Each table shows the compression strength results for a particular pallet pattern and board type.

4.2.1 Corrugated Box (SW-A)

Table 10 shows the percent compression strength loss of the SW-A corrugated box in the column type stacking pattern. The compression strength of the box before vibration averaged 806.9 lbs and the compression strengths after vibration at resonance for 15 minutes with a stack load of 105, 157.5 and 213 lbs on top averaged 666.7, 650.1, and 391.1 lbs respectively. The percent loss in compression strength using the 806.9 lb value as a reference is therefore 17.3%, 19.4%, and 51.5% respectively on average. Table 11 shows the percent compression strength loss of the SW-A corrugated box in the interlock type stacking pattern. The loss in compression strength of the SW-A averaged 17.7%, 18.3%, 19.9% for static loads of 105 lbs, 157.5 lbs, and 213 lbs respectively. Table 12 shows the percent compression strength loss of the SW-A corrugated box in the pinwheel type stacking pattern.
The loss in compression strength of the SW-A averaged 0.0%, 20.7%, 22.5% for static loads of 115 lbs, 157.5 lbs, and 213 lbs respectively.

The results in Table 10, 11,and 12 for the average

compression strengths are graphed in Figure 12. It would appear that the greater the static load, the greater the loss in compression strength. The specific loss did not seem to be related to the type of pallet pattern until the static load exceeded 157.5 lbs. Beyond 157.5 lbs, the column type stacking pattern had the highest percent loss of compression strength.

Table 10. Column Type Stacking Pattern : SW-A

No	Total Static Load (lbs)			
	0	105	157.5	213
1	666	*959	548	478
2	762	751	618	330
3	904	548	659	398
4	656	591	656	375
5	815	707	709	437
6	856	721	672	378
7	789	684	692	342
Average Compression Strength lb	806.9	667.7	650.1	391.1
STD	150.4	79.8	53.1	52.1
Resonance	No vib.	7.5Hz	7.2Hz	6.5Hz

* not included in the average.

Table 11. Interlock Type Stacking Pattern : SW-A

No	Total Static Load (lbs)			
	0	105	157.5	213
1	666	*1021	666	*1039
2	762	669	692	642
3	904	516	747	501
4	656	742	800	659
5	815	738	609	698
6	856	627	465	641
7	789	692	634	736
Average Compression Strength lb	806.9	664.0	659.0	646.2
STD	150.4	84.8	107.6	80.0
Resonance	No vib.	7.3Hz	7.0Hz	6.3Hz

* not included in the average.

Table 12. Pinwheel Type Stacking Pattern : SW-A

No	Total Static Load (lbs)			
	0	105	157.5	213
1	666	703	*1057	*1029
2	762	654	604	686
3	904	760	578	695
4	656	789	636	428
5	815	695	713	712
6	856	586	639	636
7	789	*1057	671	594
Average Compression Strength lb	806.9	711.2	640.2	625.2
STD	150.4	81.0	47.9	105.9
Resonance	No vib.	7.5Hz	7.2Hz	6.5Hz

* not included in the average.

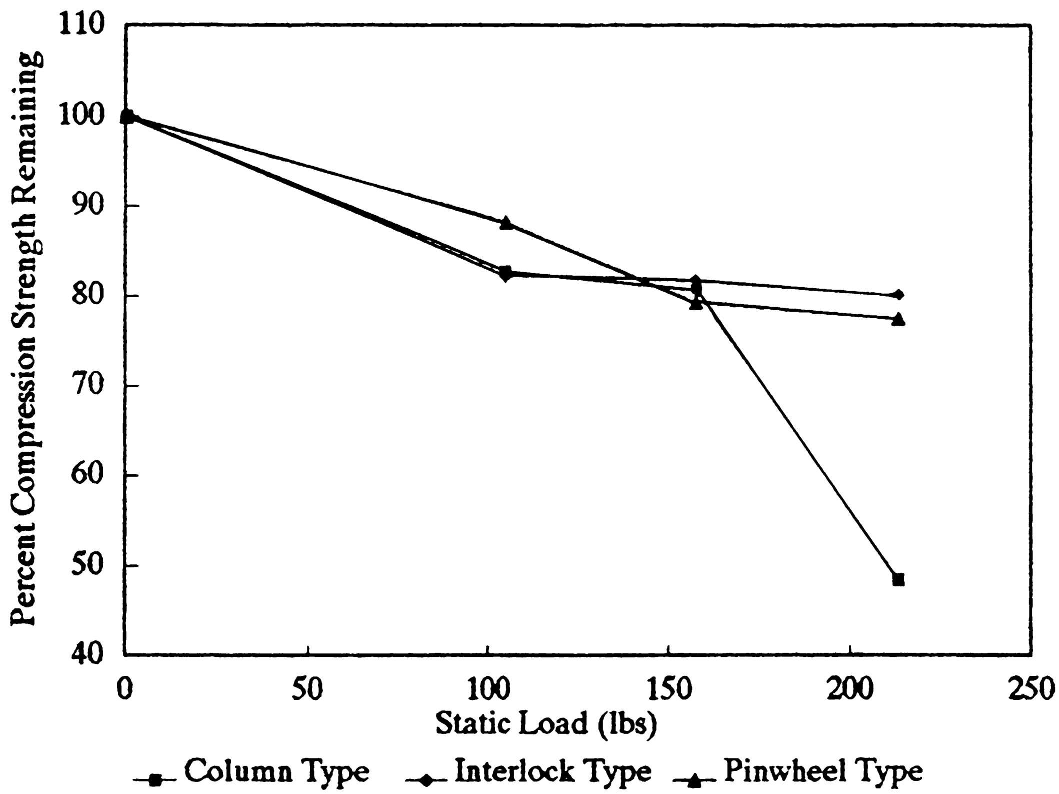

Figure 12. Mean Percent Compression Strength Remaining
: SW-A

4.2.2 Corrugated Box (SW-B)

Table 13 shows the percent compression strength loss of the SW-B corrugated box in the column type stacking pattern. The compression strength of the box before vibration averaged 1068.6 lbs and the compression strengths after vibration at resonance for 15 minutes with a stack load of 105, 157.5 and 213 lbs on top averaged 1011.3, 987.9, and 886 lbs respectively. The percent loss in compression strength using the 1068.6 lb value as a reference is therefore 0.0%, 0.0%, and 17.1% respectively on average. Table 14 shows the percent compression strength loss of the SW-B corrugated box in the interlock type stacking pattern. The loss in compression strength of the SW-B averaged 7.9%, 11.8%, 13.8% for static loads of 105 lbs, 157.5 lbs, and 213 lbs respectively. Table 15 shows the percent compression strength loss of the SW-B corrugated box in the pinwheel type stacking pattern.
The loss in compression strength of the SW-B averaged 0.0%, 12.1%, 16.2% for static loads of 115 lbs, 157.5 lbs, and 213 lbs respectively.

The results in Table 13, 14,and 15 for the average compression strengths are graphed in Figure 13. It would appear that the greater the static load, the greater the loss in compression strength. The specific loss did not seem to be related to the type of pallet pattern. But with a static load of 157.5 lbs, the column type stacking pattern had the highest percent loss of compression strength.

Table 13. Column Type Pallet Pattern : SW-B

No	Total Static Load (lbs)			
	0	105	157.5	213
1	1051	1145	929	783
2	1083	1059	921	847
3	1057	1038	1027	1088
4	1113	1056	762	1086
5	1086	959	1130	826
6	1106	918	1057	792
7	999	904	1089	780
Average Compression Strength lb	1068.6	1011.3	987.9	886.0
STD	38.4	87.4	126.3	131.3
Resonance	No vib.	7.5Hz	7.2Hz	6.5Hz

Table 14. Interlock Type Pallet Pattern : SW-B

No	Total Static Load (lbs)			
	0	105	157.5	213
1	1051	886	851	904
2	1083	898	1033	991
3	1057	906	932	951
4	1113	1045	995	862
5	1086	994	891	932
6	1106	1110	950	918
7	999	1045	943	891
Average Compression Strength lb	1068.6	984.4	942.1	921.3
STD	38.4	88.0	60.7	42.1
Resonance	No vib.	7.3Hz	7.0Hz	6.3Hz

Table 15. Pinwheel Type Pallet Pattern : SW-B

No	Total Static Load (lbs)			
	0	105	157.5	213
1	1051	1117	874	959
2	1083	1109	1041	959
3	1057	998	810	845
4	1113	1026	1039	854
5	1086	979	966	885
6	1106	1012	901	864
7	999	914	945	900
Average Compression Strength lb	1068.6	1022.1	939.4	895.1
STD	38.4	71.6	85.1	47.4
Resonance	No vib.	7.5Hz	7.2Hz	6.5Hz

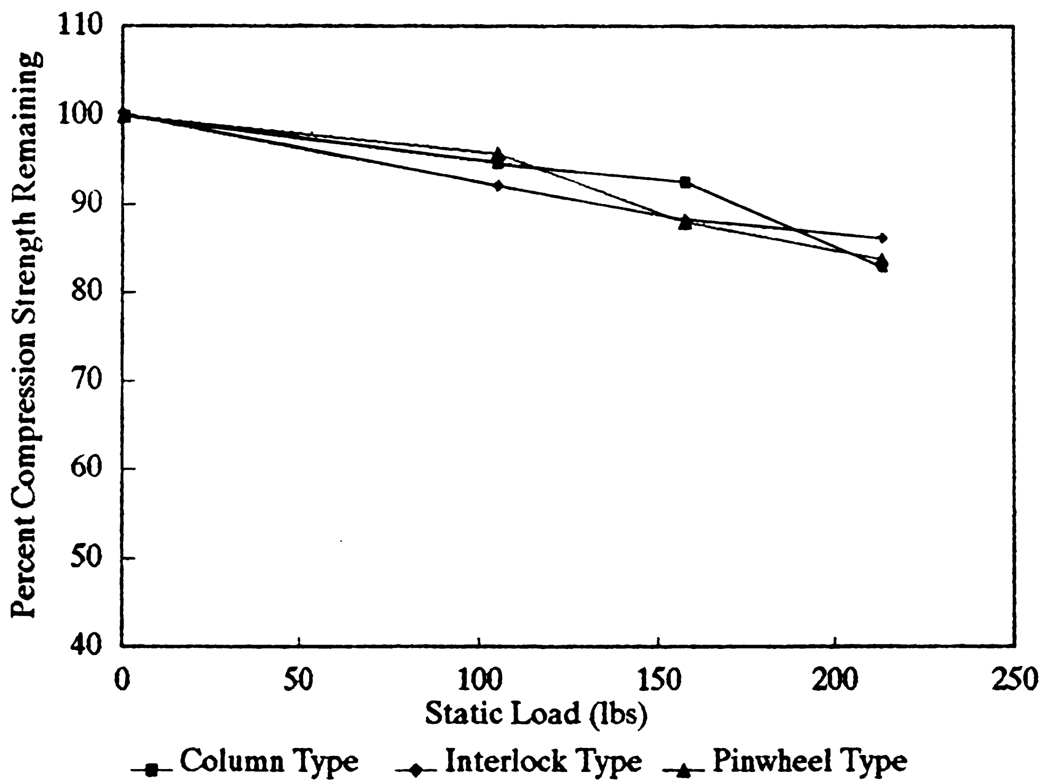

Figure 13. Mean Percent Compression Strength Remaining
: SW-B

4.2.3 Corrugated Box (DW)

Table 16 shows the percent compression strength loss of the DW corrugated box in the column type stacking pattern. The compression strength of the box before vibration averaged 1358.1 lbs and the compression strengths after vibration at resonance for 15 minutes with a stack load of 105, 157.5 and 213 lbs on top averaged 1432.6, 1300.1, and 1407.3 lbs respectively. The percent loss in compression strength using the 1068.6 lb value as a reference is therefore 0% for all three stack loads on average. Table 17 shows the percent compression strength loss of the DW corrugated box in the interlock type stacking pattern. The loss in compression strength of the DW averaged also 0% for three static loads of 105 lbs,157.5 lbs, and 213 lbs. Table 18 shows the percent compression strength loss of the DW corrugated box in the pinwheel type stacking pattern. The loss in compression strength of the DW averaged 0% again for three static loads of 115 lbs, 157.5 lbs, and 213 lbs.

The results in Table 13, 14,and 15 for the average compression strengths are graphed in Figure 14. It would appear that the compression strength of DW corrugated board box is not affected by the stacking pattern and vibration test used.

Table 16. Column Type Pallet Pattern : DW

No	Total Static Load (lbs)			
	0	105	157.5	213
1	1259	1400	1471	1364
2	1288	1529	1271	1377
3	1368	1340	1332	1505
4	1257	1424	1409	1418
5	1210	1383	1034	1336
6	1589	1448	1210	1395
7	1536	1504	1374	1456
Average Compression Strength lb	1358.1	1432.6	1300.1	1407.3
STD	148.3	66.8	145.7	57.8
Resonance	No vib.	7.5Hz	7.2Hz	6.5Hz

Table 17. Interlock Type Pallet Pattern : DW

No	Total Static Load (lbs)			
	0	105	157.5	213
1	1259	1217	1378	1300
2	1288	1373	1235	1649
3	1368	1333	1030	1306
4	1257	1362	1385	1327
5	1210	1285	1362	1326
6	1589	1471	1241	1381
7	1536	1526	1471	1443
Average Compression Strength lb	1358.1	1366.7	1300.3	1376.0
STD	148.3	105.3	145.5	123.3
Resonance	No vib.	7.3Hz	7.0Hz	6.3Hz

Table 18. Pinwheel Type Pallet Pattern : DW

No	Total Static Load (lbs)			
	0	105	157.5	213
1	1259	1377	998	1412
2	1288	1215	1514	1545
3	1368	1341	1388	1214
4	1257	1250	1301	1464
5	1210	1291	1500	1567
6	1589	1270	1409	1420
7	1536	1285	1361	1467
Average Compression Strength lb	1358.1	1289.9	1364.4	1441.3
STD	148.3	54.5	186.9	116.0
Resonance	No vib.	7.5Hz	7.2Hz	6.5Hz

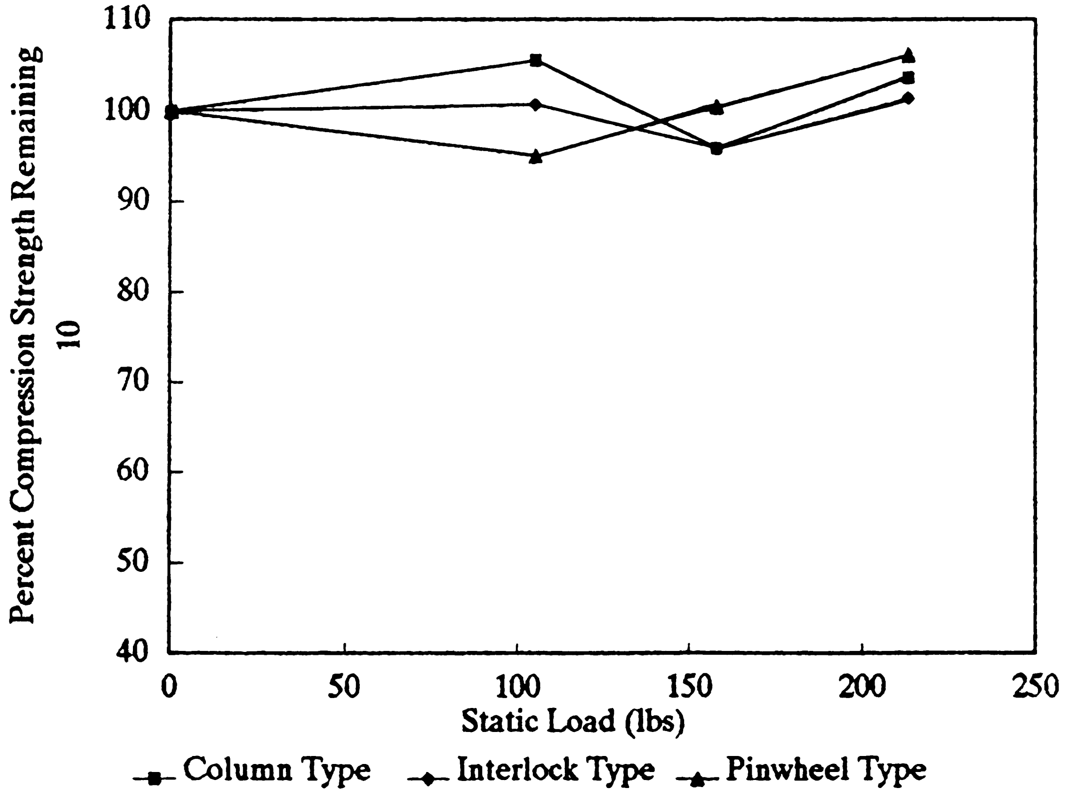

Figure 14. Mean Percent Compression Strength Remaining : DW

5.0 CONCLUSIONS

Based on the test results, the following conclusions were reached :

1. The ISB has a static and dynamic measurement error of ± 5.5 lbs and an external acceleration measurement error of ± 0.02G.

2. The percent compression strength losses of SW-A, SW-B, and DW boxes as a function of the static load expressed as a percent of the box compression strength are described in Table 19 below.

Table 19. Static load vs Compression Strength Loss

Static loads as a percent of compression strength	Percent loss in compression strength due to different stacking patterns			
		Column	Interlock	Pinwheel
13.1% 19.5% 26.4%	SW-A	17.3% 19.4% 51.5%	17.7% 18.3% 19.9%	0.0% 20.7% 22.5%
9.8% 14.7% 19.9%	SW-B	0.0% 0.0% 17.1%	7.9% 11.3% 13.8%	0.0% 12.1% 16.2%
7.7% 11.6% 15.7%	DW	No Loss		

3. According to the compression test results in Table 19 for SW-A and SW-B, the interlock type stacking pattern has the maximum compression strength loss at the lightest package weight; the pinwheel type stacking pattern has the maximum compression strength loss at the intermediate package weight; and the column type stacking pattern shows the maximum compression strength loss at the heaviest package weight. The column type pallet pattern produces the greatest loss in compression strength at higher static loads compared to the interlock and pinwheel patterns most likely because the bottom boxes are loaded primarily on their corners during vibration. Many of the corners of the bottom boxes in the pinwheel and interlock patterns contact the middle of the boxes above them (not the corners as in the column type pattern). This means that the corners of the bottom boxes are not abused as much which then leaves them stronger after vibration. Figures 7, 8, and 9 illustrate this. Since compression strength is primarily related to the strength of the corners(Maltenfort, 1988, 1989), greater loading of the corners during vibration is expected to result in a lower compression strength after vibration.

4. Because the dynamic forces on the bottom boxes never exceeded the compression strength of the box for any of the box types (SW-A, SW-B, and DW), no conclusion can be reached regarding the effect of dynamic forces on box failure. In other words, it is not known whether periodic dynamic forces

in excess of the static compression strength will cause a box to fail.

5. The use of stack resonance tests as outlined in ASTM D 999 resulted in dynamic forces up to about 2.2 times the static loads at resonance. See Tables 6, 7, and 8. Earlier studies using ASTM D 4728 (Singh and Leinberger, 1992) produced dynamic forces up to 5 times the static loads using the composite truck spectrum. Therefore, ASTM D 999 is not as severe a test as ASTM D 4728.

6. The Rule 41 recommendations on gross weight were found to be valid. The greatest static load placed on any of the boxes was 213 lbs. This was due to the three 71 lb boxes on top of it. According to Table 4, this box weight exceeded the Rule 41 recommendation of 65 lbs only for the SW-A box. The SW-A boxes with 213 lb static load on top should therefore have shown the greatest amount of damage and presumably the greatest loss in compression strength. According to Figure 12, this was in fact the case.

7. Based on Newton's law, dynamic forces can be accurately predicted by measuring accelerations provided that there is no separation between the stack of boxes during vibration. The dynamic compression levels at resonance where the boxes separate and bounce can not be predicted. Therefore, the ISB can not be replaced by accelerometers during transit if resonance conditions are expected.

List of References

Antle, John Rodney. 1989. Measurement of Lateral and Longitudinal Vibration in Commercial truck Shipments. MSU: School of Packaging.

ASTM. 1991. Selected ASTM Standards on Packaging. Philadelphia, PA: ASTM.

Blatt, Frank . 1986. Principles of Physics. Massachusetts: Ally and Bacon Inc.

Brandenburg, Richard K., Lee, Julian June-Ling. 1985. Fundamentals of Packaging Dynamics. USA: MTS System Co.

Dority, Jack. 1989. Solving Distribution Damage Problems in the Laboratory. Journal of Packaging Technology. Vol. 3. No. 1:pp13-16.

Fibre Box Association. 1989. Fibre Box Handbook. Rollong Meadows,IL: Fibre Box Association.

Harris, Cyril M and Crede, Charles E. 1976. Shock and Vibration Handbook. USA: Mcgraw-Hill Inc.

Maltenfort, George G. 1988. Corrugated Shipping Containers. Plainview, NY: Jelmar Publishing Co., Inc.

Maltenfort, George G. 1989. Performance and Evaluation of Shipping Containers. Plainview, NY: Jelmar Publishing Co., Inc.

Marcondes, Jorge Aparecido. 1988. Dynamic Analysis of a Less Than Truckload Shipment. MSU: School of Packaging.

Singh, Paul and Leinberge, Dave. 1993. Identification of Methodology, Equipment, and Software necessary to Perform Environmental Data Acquisition of Dynamic Compression Values on Individual Packages in Shipment. MSU: School of packaging.

Timoshenko, S., Young, D.H., and Weaver, JR. W. 1974. Vibration Problems in Engineering (Forth Edition). New York:

John Wiley & Sons.

Wiley. 1986. Mechanical Engineers' Handbook. New York: Wiley.

Wilson, T Douglas. 1988. How Cushion Packaging Design Can Control Vibration Damage During Transport. Journal of Packaging Technology. Vol. 2. No. 3:pp106-108.

APPENDIX

INSTRUMENTED SHIPPING BOX

Technical Description of Instrumented Shipping Box :

The instrumented shipping box consisted of the following main items, (these items were installed in a 13"width, 16" length by 10" tall box sized to approximate a standard shipping container).

1. One, 8-bit controller style microprocessor containing 64K of non-volatile static ram, a real-time clock calendar, both a synchronous and asynchronous serial port, and a lithium backup battery.

2. Four, 8-megabyte dynamic ram storage (mass storage) memory banks. These memory devices used synchronous serial to communicate with the microprocessor.

3. Two, 8-channel multiplexed twelve-bit analog to digital converters (A/D). The A/D used synchronous serial to communicate with the microprocessor.

4. Four, instrumentation amplifiers to process the signal from the sheer beams.

5. Four, 0-5000lb. shear beam style load cells. These load cells were temperature compensated from 0 to 150 degrees fahrenheit, were 3 mV/V signal at full output, and used a 350 ohm bridge resistance.

6. One, 0-±50g monolithic capacitive accelerometer. The sensitivity was approximately 20 mV/V signal with a full frequency response from 0 Hz. to 500 Hz (3db down). The range of the accelerometer was limited to ± 20gs.

7. Two, 4amp/hour 6 volt lead acid, gel type batteries.

8. A hexademical rotary input switch to control the mode of operation. Two push button switches to increment, decrement, or commence the function of a given mode.

9. A RS232 style serial port (9600 baud) to send or receive information from a PC computer.

10. Three power suppliers, one five volt supply for the digital circuitry, one eight volt supply for the analog circuitry, and one precision five volt supply for the A/D. A crowbar was used to protect the circuitry against overvoltage.

11. A built-in battery charge for the gel batteries. The batteries can be recharged in approximately five hours. A two color led indicates the condition of charging (red=charging, green = full charge). The box could run for approximately 20 hours on a full charge.

12. A 16x2 full alpha-numeric liquid crystal display (LCD) was used to provide information to the box user.

<u>Explanation of Features :</u>

The four load cells were placed at each corner of the boxes lid. The lid was undercut so that it could float free of the box sides and was supported by the load cells. With this type of arrangement the forces acting on individual corners could be measured (0-5000lb.) as well as the sum of the forces on the entire lid (20000lb.). The box was constructed of 5/8th" plywood with the lid from 3/4" plywood. The maximum test force placed on the box (to date) was 3000+lb. The load cells were supported on the internal steel box-beam frame that provided rigid support and overload protection. The lid could be removed and a smaller lid version placed on an individual corner to test the accuracy of a given load cell.

The microprocessor used an 11.0592 Mega-Hz. crystal resulting in a machine cycle time of 1.1Us. This crystal frequency provided both the highest processor speed and allowed the development of special timing for the asynchronous serial port. The real-time clock calendar provided a means of time/date stamping test runs. The lithium backup battery provided by the retention of microprocessors programs and data without the need for EPROM or EEPROM type memory. The bulk of the test data was stored in the mass storage devices. A means of testing the mass storage for stuck bits was provided. The LCD provided an independent means of viewing the lid weights, box temperatures, battery charge, and amount of mass storage filled.

The two A/Ds provided a total of sixteen channels of 12-bit data acquisition. A/D #1 provided information from the four sheer beams, monitored the analog voltage supply, the 12V battery pack, and two temperatures (sheer beam and box ambient). A/D #2 provided information from the single axis accelerometer and would allow for future expansion. Due to the amount of time it took to access the A/Ds are saved the information in mass storage a maximum sampling time of 200 Hz. was achieved. For convenience and due to different testing

criteria the sample rate could be incrementally varied from 0.1 Hz to 200 Hz. To read and save data from one channel of an A/D required approximately 0.275 ms. To provide the most "instantaneous" reading of the A/D channels, they were red in a burst mode at the beginning of a sample cycle saving the data to the microprocessor to the mass storage. At 200 Hz the mass storage could be filled in approximately 21 minutes.

A typical data gathering session would proceed as follows.

The user turns the box on and lets it "warm-up" for five to ten minutes.During this time the sampling rate is set and at the end of this time a tare weight is taken. When the box is put in the data gathering mode a file heading is created that records the start time and date, the sample rate, the zero value for the accelerometer. As data is gathered it is saved, along with a check sum, in the mess storage. One sample of all the A/D channels is one packet and has a one-byte check sum. At the end of a data gathering session the number of packets is added to the header information.

The instrumented box is turned on a serial download mode and connected to a PC to transfer the data. The header information provides the program in the PC with the number of packets of information to receive, and necessary consultants to recreate the actual information. Storing raw data in the instrumented box allows for faster sampling time and more efficient use of the mass storage. Providing a check sum with

each packet provided a means of checking data integrity.